Ambient-Condition nano-Alumina Formation Through Molecular Control

Yuzhong Wang[a], Sonali Bhandari[a], Amitabha Mitra[a], Sean Parkin[a], Jerry Moore[b], and David A. Atwood[a,*]

[a] Lexington, KY/ U.S.A., University of Kentucky, Department of Chemistry
[b] Argonne, IL / U. S. A., Argonne National Laboratory, Materials Science Division 60439

Received December 27th, 2004.

Dedicated to Professor Herbert W. Roesky on the Occasion of his 70th Birthday

Abstract. When toluene solutions of the tetrametallic compound, $[Al\{\mu\text{-}OEt)_2AlMe_2\}_3]$ (**1**), are stirred in air at room temperature, pure amorphous nanoparticulate Al_2O_3 precipitates. The average particle size is 17.7 ± 7.4 nm. The tetrametallic core of **1**, having the correct stoichiometry for alumina ($2Al_2O_3$) appears to act as a template or nucleating site for the formation of alumina rather than the expected products of formula, AlOOH. The stability of the Al_4O_6 core of **1** was tested by combining it with six equivalents of Ph_3SiOH. This resulted in $[Al\{\mu\text{-}OEt)_2Al(OSiPh_3)_2\}_3]$ (**2**). Upon exposure to air, compound **2** formed the hydroxide derivative $[Al\{\mu\text{-}OH)_2Al(OSiPh_3)_2\}_3]$ (**3**). This demonstrates that the tetrametallic core of **1** is stable to both peripheral derivatization as well as alcoholysis of the internal bridging groups.

Keywords: Alkoxide; Aluminum; Alumina; Mitsubishi structure; Tetrametallic

Introduction

Over the past several years, there has been increasing interest in molecular routes to materials [1]. Stoichiometric single source molecular precursors are appealing because they favor more intimate mixing of the elements, enable the reactions to take place at lower temperatures than other routes, or allow access to more pure or otherwise inaccessible phases. In particular, synthetic routes to nanoparticulate materials would be of great technological value [2]. The recent discovery of the unusual reactivities and structural properties of nanostructured materials has led to enhanced research in the synthesis of such materials by entirely new approaches or by modifying older methods [3]. The unusual electronic and catalytic properties of nanostructured materials render them particularly interesting [3]. Stoichiometric precursors to Group 13/16 materials requiring a 13/16 ratio of 2:3, suitable for the formation of Al_2O_3 for example, are extremely rare. In general, the known precursors to this material have simply used an excess of oxygen, in combination with an aluminum alkoxide or carboxylate. For example, $Al(acac)_3$ [4], $Al(OOR)_3$ [5], $Al(OR)_3$ [6], $R_2Al(OR)$ [7], and $R_2Al(acac)$ [8] (R = alkyl) have been used to prepare aluminum oxide thin films. Bulk quantities of pure alumina are accessible only through high temperature syntheses [9]. Precedents of powdered nanoalumina formation from aluminum ethoxide [10], aluminum tri-*tert*-butoxide [11], aluminum isopropoxide and aluminum tributoxide precursors exist in the literature. These studies have shown that variation of starting material, type and amount of solvent and stirring time have an effect on the surface properties of the alumina. *Kung* et al. have recently proven that a controlled synthesis can affect the surface properties of alumina [12]. The strategy employed in this study is to cap the Lewis acid sites of alumina with a base during hydrolysis to form the oxide. The bound amine can then be exchanged with other bases. Alumina synthesized using piperidine as the base was found to be a catalyst for the aminolysis of epoxide by amine, [13] a class of reactions that have potential in drug synthesis [14].

Recently, our group reported a series of tetrametallic molecules $[Al\{\mu\text{-}OEt)_2AlR_2\}_3]$ (R = Me (**1**), Et, ^{i}Bu) with a tri-diamond or "Mitsubishi™" structure [15, 16]. These molecules were designed for creating corrosion resistant coatings on metal substrates [17]. The molecules were thought to diffuse into the corrugated surface of the metals and, with heating, decompose to Al_2O_3 in the absence of additional reagents.

In this publication we report the remarkable discovery that these tri-diamond molecules hydrolyze in air to form pure alumina, Al_2O_3 (rather than boehmite or gibbsite). The alumina is amorphous based upon XRD (powder X-ray diffraction) but pure based on EDX (Energy Dispersive X-ray analysis). Importantly the material was nanoparticulate with an average particle size of 17.7 ± 7.4 nm and a surface area of 108.82 $m^2.g^{-1}$ (BET). Additionally, elemental analysis demonstrates that there is no significant carbon or hydrogen contamination (< 0.5 %).

Results and Discussion

Preparation of $[Al\{\mu\text{-}OEt)_2Al(OSiPh_3)_2\}_3]$ (2) *and $[Al\{\mu\text{-}OH)_2Al(OSiPh_3)_2\}_3]$* (3)

A series of tetrametallic D_3-Symmetric alkoxide molecules containing aluminum of general formula $[Al\{(\mu\text{-}OEt_2AlR_2\}_3]$

* Prof. David A. Atwood
Department of Chemsitry
University of Kentucky
Lexington, KY 40506, USA
E-mail: datwood@uky.edu
Fax: 1-859-323-1069

where R = Me (**1**), Et and ^{i}Bu have been previously synthesized and fully characterized in our laboratory [15, 16]. To explore the stability of the Al_4O_6 core, **1** was combined with 6 equivalents of tri(phenyl)silanol (Scheme 1). The result was a 76 % yield of $[Al\{\mu\text{-}OEt)_2Al(OSiPh_3)_2\}_3]$ (**2**), the only aluminum-containing product that could be isolated from the reaction. The Al_4O_6 core of **1** is also present in compound **2**. The ethoxide groups do not redistribute in the presence of tri(phenyl)silanol as observed when an aluminum alkoxide and silanol are combined [18]. Compound **2** hydrolyzed upon exposure to air to form the hydroxide derivative $[Al\{\mu\text{-}OH)_2Al(OSiPh_3)_2\}_3]$ (**3**) (Scheme 1). The fact that water does not displace the tri(phenyl)silanol ligands as it does the alkyl groups in the formation of alumina from **1** can be explained by the greater acidity of $HOSiPh_3$ (pKa, 10.8) compared to water [19].

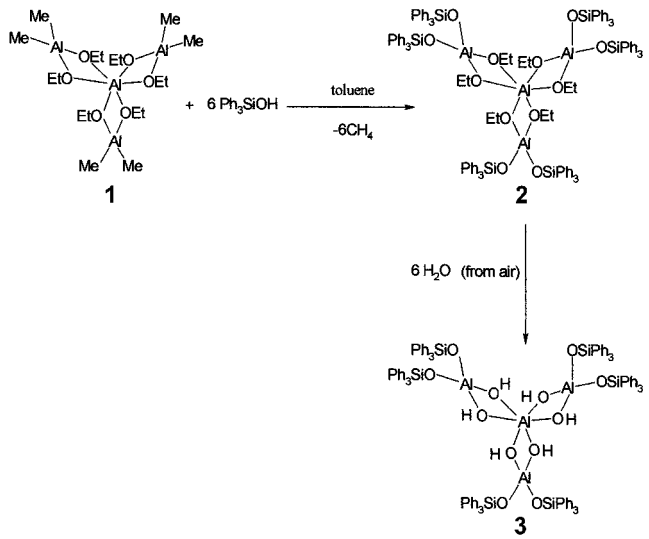

Scheme 1 Compound **1** reacts with tri(phenyl)silanol to form compound **2**. Compound **2** hydrolyzes to compound **3**.

Characterization of $[Al\{\mu\text{-}OEt)_2Al(OSiPh_3)_2\}_3]$ (2) *and* $[Al\{\mu\text{-}OH)_2Al(OSiPh_3)_2\}_3]$ (3)

Like **1**, compounds **2** and **3** maintain their tetrametallic structures in solution (based on NMR and reactivity). The stability of the tetrametallic structure in solution can be attributed to the exceptional strength of the combined Al−O−Al bridges [20]. Compounds **2** and **3** were characterized by ^{1}H NMR, ^{27}Al NMR, elemental analysis, IR and mass spectrometry (MALDI). The mass spectrum (EI, positive) of compound **3** contains two important peaks: 78 (100.0 %, $[Al(OH)_3]^+$), 1267 (1.0 % $[Al\{(\mu\text{-}OH)_2Al(OSiPh_3)_2\}_3 - Al(OH)(OSiPh_3)_2]^+$) that support the proposed structure (Scheme 1).

Description of the crystal structure of $[Al\{\mu\text{-}OEt)_2Al(OSiPh_3)_2\}_3]$ (2)

Compound **2** crystallizes as a monomer from CH_2Cl_2 solution (Fig. 1). The structure is similar to that of

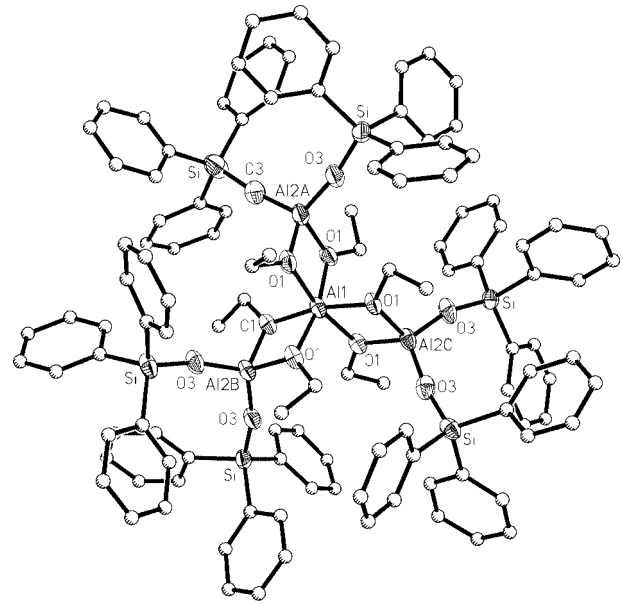

Figure 1 Molecular structure of $[Al\{\mu\text{-}OEt)_2Al(OSiPh_3)_2\}_3]$ (**2**)

Selected bond distances/Å and angles/°: Al1-O1A 1.902(4), Al1-O2A 1.896(4), Al1-O1B 1.903(4), Al1-O2B 1.907(4), Al1-O1C 1.917(4), Al1-O2C 1.898(4), Al2A-O1A 1.792(4), Al2A-O2A 1.789(5), Al2BO1B 1.792(4), Al2B-O2B 1.794(4), Al2C-O1C 1.796(4), Al2CO2C 1.786(4), Si1A-O3A 1.601(5), Si2A-O4A 1.609(5), Si1BO3B 1.610(4), Si2B-O4B 1.612(5), Si1C-O3C 1.617(4), Si2CO4C 1.608(4), Si1A-O3A-Al2A 173.0(3), Si2A-O4A-Al2A 170.0(3), Si1B-O3B-Al2B 162.7(3), Si2B-O4B-Al2B 169.3(3); Si1C-O3C-Al2C 163.7(3), Si2C-O4C-Al2C 164.2(3).

$[Al\{\mu\text{-}OEt)_2AlR_2\}_3]$ (R = Me (**1**), Et) which also exhibit a tetrametallic tri-diamond structural motif [15, 16]. Compound **2** contains one central six-coordinate aluminum and three four-coordinate aluminum atoms connected to the central atom through six bridging oxygen atoms. Also, like the $[Al\{\mu\text{-}OEt)_2AlR_2\}_3]$ (R = Me (**1**), Et) structures, the Al−O distances are longer around the central six-coordinate aluminum atom (av. 1.9 Å) than for the four-coordinate aluminum atoms (av. 1.8 Å); this is expected as the atomic radii increase with an increase in coordination number [15, 16]. The Si−O bond distances, ranging from 1.601(5) Å to 1.617(4) Å, are comparable to those observed in several related compounds [20, 21]. The Al−O($SiPh_3$) bond distances (1.692(4) Å−1.701(4) Å) are comparable to those in the previously reported Al−$(OSiPh_3)_3$(THF) (1.696(4) Å, 1.703(4) Å, and 1.709(4) Å) [22].

Decomposition of $[Al\{\mu\text{-}OEt)_2AlMe_2\}_3]$ (1)

When 2 g of **1** was stirred in 500 mL of dry toluene at room temperature for one month open to air, a fine white powder was obtained (Scheme 2). Characterization studies revealed that the fine white powder was nano-alumina. This nano-alumina was formed by the hydrolysis of **1** by moisture absorbed from the air. In the absence of further studies the complete pathway for the hydrolysis reaction could not be

ascertained but the initial step was very likely to be the cleavage of alkyl- aluminum bonds by H_2O.

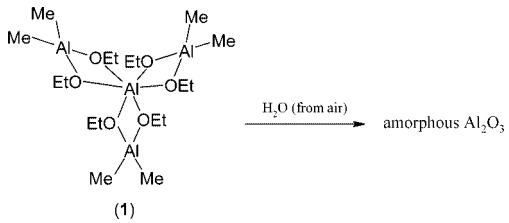

Scheme 2 Compound **1** decomposes to amorphous alumina.

Characterization of the Aluminum Oxide

TGA (thermogravimetric analysis) of the alumina revealed two weight loss regions. The weight loss of 38.6 % between 0 °C and 250 °C was due to desorption of water and organic contaminants (Benzene, 1-methyl-2-[(3-methylphenyl)methyl]) as observed by gc/ms. The weight loss of 0.57 % in the 850−930 °C range can be attributed to the transformation of amorphous to crystalline alumina. The absence of weight loss in the 250−800 °C range rules out the presence of chemisorbed water [23].

Table 1 X-ray diffraction results of alumina samples after heating for two hours at different temperatures

Temperature	Phase
600 °C	Amorphous alumina
800 °C	Amorphous alumina + γ-alumina
1000 °C	Amorphous + θ + γ-alumina
1100 °C	α + θ + γ-alumina
1200 °C	Mainly α-alumina + traces of θ-alumina

Table 2 Decomposition sequence of aluminum hydroxides [26]

Aluminum Hydroxide	Decomposition Sequence
Gibbsite	CHI (300-500 °C) − KAPPA (800-1150 °C) − ALPHA (1150 °C −)
Boehmite	GAMMA (500 − 850 °C) − DELTA (850-1050 °C) − THETA (1050 − 1150 °C) − ALPHA (1150 °C −)
Bayerite	ETA (300 − 500 °C) − THETA (880 − 1150 °C) − ALPHA (1150 °C−)
Diaspore	ALPHA (500 °C−)

Remarkably, the XRD data (Table 1) indicate that the alumina remains amorphous up to 800 °C. Crystallization observable by XRD only occurs between 800 and 1000 °C. This corresponds to the transformation of amorphous alumina to a crystalline phase and is consistent with the TGA results. At 1000−1200 °C, α- and θ-alumina are observed. These observations are in sharp contrast to the XRD powder patterns obtained from thermal evolution of transitional aluminas obtained from boehmite [24−26], bayerite [24, 25], gibbsite [25] and other conventional amorphous alumina as depicted in Table 2 [26]. Transformation of the alumina in the current study to crystalline phases at much higher temperatures than those reported in the literature suggest the presence of a highly structured core that requires high temperatures for rearrangement.

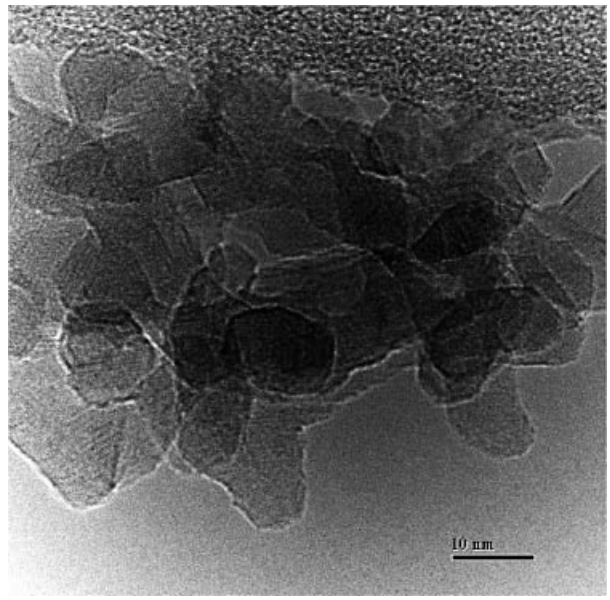

Figure 2 TEM image of Al_2O_3 formed from the decomposition of compound **1**.

The TEM image (Fig. 2) of the alumina shows the average particle size of 17.7 ± 7.4 nm and BET studies give a surface area of 108.82 $m^2.g^{-1}$. These data confirm the nanoparticulate nature of the alumina formed.

Solid-state ^{27}Al NMR reveals peaks at 10.9, 41.0 and 75.5 ppm corresponding to 6-, 5- and 4- coordinate Al environments, respectively. The appearance of three coordination environments for Al is consistent with other known amorphous aluminas [27]. Whereas the solid-state ^{27}Al NMR for boehmite [28], bayerite [29] and α-alumina [28] exhibit only six-coordinate Al, Gibbsite [30] and γ-alumina [28] exhibit six- and four- coordinate Al environments. An infrared absorption spectrum of the fine white amorphous material reveals a broad band at 500−1000 cm^{-1}, which is characteristic of amorphous nano-Al_2O_3. [26]. In addition, an unresolved broad band in the range 2900−3700 cm^{-1} is also observed, which can be assigned to hydrogen-bonded hydroxyls, present at the surface of the solid [31]. However, structural hydroxyls attributable to boehmite (1155(sh) cm^{-1} and 1065(vs) cm^{-1}) [30] and gibbsite (1034(m) cm^{-1} and 980(vs) cm^{-1}) [32] were clearly not present. Raman spectrum reveals peaks at 550 and 1100cm^{-1}. This is markedly different from other crystalline or hydrated aluminas [33].

In contrast with the alumina formation observed for **1**, the hydrolysis of other known alkyl aluminum compounds produces boehmite (AlOOH) [34]. The tetrametallics used here clearly undergo some form of hydrolysis but not to the

expected hydrolytic product, AlOOH. This may be attributed to the pre-assembled core of aluminum and oxygen atoms that apparently pre-ordain the elements involved to form alumina rather than boehmite. The core, in effect, acts as a template for the formation of new Al−O (alumina) bonds.

Experimental Part

The decomposition of **1** and the characterization of the alumina were carried out in air. All other manipulations were conducted using Schlenk techniques and an inert atmosphere glove box. All solvents were rigorously dried prior to use. All glassware was cleaned with a base and an acid wash and dried in an oven at 130 °C overnight prior to use. NMR data were obtained on JEOL-GSX-400 and −270 instruments at 270.17 (^{1}H) and 104.5 (^{27}Al) MHz. Chemical shifts are reported relative to $SiMe_4$ and are in ppm. ^{27}Al magic angle spinning (MAS) NMR spectra were acquired at 104 MHz (9.4T) on a Varian 400 MHz Inova spectrometer with a spinning rate of 8 KHz. Pulse width in the range of 1.2 to 3μs was used together with recycle time ranging from 6-15s. $Al(NO_3)_3$ was used as the reference. Elemental analyses were obtained on a Perkin-Elmer 2400 analyzer and were found to be within acceptable limits for **2** and **3**. Infrared data were recorded as KBr pellets on a Matheson Instruments2020 Galaxy Series spectrometer and are reported in cm^{-1}. Brunauer-Emmet-Teller (BET) surface area was measured on Micromeritics ASAP 2000 Accelerated Surface Area and Porosimetry Analyzer. Thermogravimetric analyses were performed on TA Instruments Hi-Res TGA 2950 Analyzer. X-ray powder diffraction data were collected on Rigaku diffractometer using CuK_α radiation. The working conditions were 40 kV and 20 mA. The presence of different phases was confirmed by comparing the XRD patterns obtained with those in JADE ICDD PDF database. R_3Al, $Al(OEt)_3$ and Ph_3SiOH were purchased from Aldrich or Strem and used as received. **Caution!** R_3Al is highly pyrophoric and must be handled under an inert atmosphere.

Synthesis of [Al{(μ-OEt)$_2$Al(OSiPh$_3$)$_2$}$_3$] (2). To a suspension of Ph_3SiOH (3.540 g, 12.8 mmol) in toluene (25 mL) at room temperature was added a toluene solution (15 mL) of [Al{(μ-OEt)$_2$AlMe$_2$}$_3$] (1.000 g, 2.13 mmol) (prepared according to the literature) [15]. After the solution was stirred for 3 days, a white precipitate formed which was isolated by filtration. It was subsequently recrystallized from CH_2Cl_2 at room temperature. **Yield:** 3.28 g (75.7 %) **Mp:** 174−176 °C. **Anal.** Calcd: C, 70.98; H, 5.96. Found: C, 70.73; H, 5.85 %.

^{1}H NMR ($CDCl_3$, 200 MHz): δ 0.49 (t, 18H, OCH_2CH_3), 3.24 (m, 6H, OCH_aH_b), 3.52(m, 6H, OCH_aH_b), 6.99−7.53 (m, 90H, Ph*H*). **^{27}Al NMR** ($CDCl_3$, 52.1 MHz): δ 58.3($\omega_{1/2}$=2288 Hz), 5.3($\omega_{1/2}$=312 Hz). **IR**(KBr; ν, cm^{-1}): 3067(m), 3048(m), 2998(w), 2977(w), 2904(w), 1960(w), 1890(w), 1825(w), 1765(w), 1654(w), 1589(w), 1485(w), 1428(s), 1305(w), 1260(w), 1187(w), 1115(s), 1060(s), 1026(m), 998(m), 900(m), 744(m), 707(s), 660(m), 620(w), 516(s). **MS** (MALDI, positive): m/z = 1363 (68.0 %, [Al{(μ-OEt)$_2$Al(OSiPh$_3$)$_2$}$_2$]$^+$), 1755 (2.0 %, [Al{(μ-OEt)$_2$Al(OSiPh$_3$)$_2$}$_3$-OSiPh$_3$]$^+$).

Synthesis of [Al{(μ-OH)$_2$Al(OSiPh$_3$)$_2$}$_3$] (3). Al{(μ-OEt)$_2$Al-(OSiPh$_3$)$_2$}$_3$ **(2)** (1.000 g, 0.49 mmol) was dissolved in CH_2Cl_2 (100 mL) and permitted to stir exposed to air until the solvent was evaporated totally. A white residue was obtained. **Yield**: (0.889 g, 96.9 %). Mp: 64−68 °C.

^{1}H NMR ($CDCl_3$, 200 MHz): δ 2.73 (br S, 6H, Al−O*H*−Al), 6.94−7.65 (m, 90H, Ph*H*); **^{27}Al NMR** ($CDCl_3$, 52.1 MHz, +70 °C): δ 66.1 ($\omega_{1/2}$=2340 Hz), 7.8 ($\omega_{1/2}$=780 Hz); **^{27}Al NMR** (MAS-NMR, 104.29 MHz): δ 59.0, 11.0. **IR** (KBr; ν, cm^{-1}): 3629(m), 3431(m), 3067(m), 3047(m), 3021(m), 1960(w), 1890(w), 1824(w), 1765(w), 1654(w), 1589(m), 1485(m), 1428(s), 1305(w), 1262(w), 1188(w), 1118(s), 1062(s), 1025(s), 997(m), 878(w), 857(w), 829(w), 741(m), 711(s), 699(s), 661(m). **MS** (EI, positive): m/z = 78 (100.0 %, [Al(OH)$_3$]$^+$), 1190 (4.0 %, [Al{(μ-OH)$_2$Al(OSiPh$_3$)$_2$}$_3$-Al(OH)(OSiPh$_3$)$_2$-Ph]$^+$), 1267 (1.0 %, [Al{(μ-OH)$_2$Al(OSiPh$_3$)$_2$}$_3$-Al(OH)(OSiPh$_3$)$_2$]$^+$).

*Decomposition of **1** to produce Nano-Alumina Particles.* To 2 g of **1** in a 1 L Schlenk flask was added 500 mL of dry toluene and the solution was stirred. After two weeks of stirring open to the air **1** formed a colloidal suspension. The solvent was then removed under vacuum to obtain a white powder. **IR** (KBr, cm^{-1}): 3506(s), 2964(w), 1558(w), 1457(w), 1263(m), 1072(w), 1004(w), 801(s). **^{27}Al NMR** (MAS-NMR, 104.29 MHz): δ 75.54, 41.06, 10.99. **Raman** (cm^{-1}): 550, 1100. **Brunauer-Emmet-Teller** (BET): 108.82 $m^2.g^{-1}$ **Transmission Electron Microscopy** (TEM): See Figure 1. **Thermogravimetric analysis (TGA)**: A weight loss of 38.6 % was observed between 0 °C and 250 °C. No change was observed in the temperature range of 250−850 °C. There was a 0.57 % drop in the weight in the 850−930 °C.

X-Ray Experimental Data for 2

X-ray quality crystals of **2** were obtained by recrystallization from CH_2Cl_2. X-ray data for **2** was collected on a Nonius Kappa-CCD unit using Mo-Kα radiation. Crystal data is summarized in Table 2. All calculations were performed using Siemens software package SHELXTL-Plus. The structures were solved by direct methods and successive interpretation of difference Fourier maps, followed by least-squares refinement. All non-hydrogen atoms were refined anisotropically. The hydrogen atoms were included in refinement in calculated positions using fixed isotropic parameters. Crystallographic data for **2** have been deposited with the Cambridge Crystallographic Data Center (CCDC reference number 219744 and copies of the data can be obtained free of charge on application to CCDC, 12 Union Road, Cambridge CB2 1EZ, UK (Fax: +44-1223-336033, e-mail: deposit@ccdc.cam.ac.uk).

Table 3 Crystal data and structure refinement for **2**

Empirical formula	C_{120} H_{120} Al_4 O_{12} Si_6
M/ g mol^{-1}	2030.67
Color	colorless
Crystal size/ mm	0.34 x 0.22 x 0.20
Crystal system	monoclinic
Space group	P 2_1/n
a/ Å	15.091(3)
b/ Å	38.495(8)
c/ Å	23.174(5)
β/ °	92.94(3)
V/ $Å^3$	13445(5)
ρ_{calc}/ g cm^{-3}	1.230
Z	4
F(000)	5193
μ (Mo-K_α) /mm^{-1}	0.343
T/ K	173(1)
hkl range	−16≤h≤16, −41≤k≤41, −24≤l≤24
Θ range/ °	1.73-22.46
Reflections measured	34495
Unique reflections (R_{int})	17464 (0.0441)
Obsd reflections, n [F≥ 4σ (F)]	12256
Refinement method	Full-matrix least-squares on F^2
Refined parameters/restraints	1767/6250
R1 [I > 2σ]	0.1028, wR2 = 0.2652
R1 (all data)	0.1391, wR2 = 0.2888
Goodness-of-fit on F^2	1.061
Largest diff. peak and hole/ e. $Å^{-3}$	0.884 and 0.704

Conclusions

We have introduced a group of stoichiometric molecular precursors that possess a pre-existing framework related to the desired Al_2O_3 solid-state material. The low-temperature atmospheric decomposition to form alumina rather than a hydrated alumina, such as boehmite, is a phenomenon that warrants further study. We are currently exploring similar precursors for mixed-metal chalcogenides, as well as other transition metal containing derivatives of compound **1** for use as precursors to new composite materials.

Acknowledgements. We thank the Office of Naval Research for financial support of this research. NMR instruments used in this research were obtained from the CRIF program of the National Science Foundation (CHE 997841) and from the Research Challenge Trust Fund of the University of Kentucky. Thanks are expressed to the MRI program of the NSF(DMR-9977388). The authors would also like to thank Professor Dibakar Bhattacharya for the BET surface area measurements, the University of Kentucky Mass Spectrometry Facility and Environmental Research and Training Laboratory (ERTL) for mass spectra.

References

[1] Some recent examples: J. Kim, B. Chen, T. M. Reineke, H. Li, M. Eddaoudi, D. B. Moler, M. O'Keeffe, O. M. Yaghi, *J. Am. Chem. Soc.* **2001**, *123,* 8239; E. G. Tulsky, J. R. Long, *Chem. Mater.* **2001**, *13*, 1149; P. A. Berseth, J. J. Sokol, M. P. Shores, J. L. Heinrich, J. R. Long, *J. Am. Chem. Soc.* **2000**, *122*, 9655; M. Lazell, P. O'Brien, D. J. Otway, J.-H. Park, *J. Chem. Soc. Dalton Trans.* **2000**, 4479; M. M. Banaszak Holl, P. T. Wolczanski, D. Proserpio, A. Bielecki, D. B. Zax, *Chem. Mater.* **1996**, *8*, 2468; J. A. Jegier, W. L. Gladfelter, *Coord. Chem. Rev.* **2000**, *206–207*, 631; O. Kahn, *Acc. Chem. Res.* **2000**, *33*, 647; J. S. Matthews, W. S. Rees, Jr., *Adv. Inorg. Chem.* **2000**; R. J. P. Corriu, *Angew. Chem.* **2000**, *112*, *Angew. Chem. Int. Ed. Engl.* **2000**, *39*, 1376; W. R. Entley, G. S. Girolami, *Science* **1995**, *268*, 397.

[2] K. J. Klabunde (ed.), *Nanoscale Materials in Chemistry*, John Wiley Sons, Inc., New York, 2001.

[3] J. Y. Ying (ed.), *Nanostructured Materials*, Academic Press, New York, 2001.

[4] M. Pulver, W. Nemetz, G. Wahl, *Surf. Coat. Technol.* **2000**, *125*, 400; D. Temple, A. Reisman, *J. Electron. Mater.* **1990**, *19*, 995; J. S. Kim, H. A. Marzouk, P. J. Reucroft, J. D. Robertson, C. E. Hamrin, Jr., *Appl. Phys. Lett.* **1993**, *62*, 681.

[5] T. Maruyama, T. Nakai, *Appl. Phys. Lett.* **1991**, *58*, 2079.

[6] V. A. C. Haanappel, J. B. Rem, H. D. van Corbach, T. Fransen, P. J. Gellings, *Surf. Coat. Technol.* **1995**, *72*, 1; H. D. van Corbach, V. A. C. Haanappel, T. G. Fransen, P. J. Gellings, *Thin Solid Films* **1994**, *239*, 31; J. Saraie, K. Ono, S. Takeuchi, *J. Electrochem. Soc.* **1989**, *136*, 3139; G. Pauer, H. Altena, B. Lux, *Int. J. Refract. Hard Met.* **1986**, *5*, 165.

[7] D. Barreca, G. A. Battiston, R. Gerbasi, E. Tondello, *J. Mater. Chem.* **2000**, *10*, 2127; W. Koh, S.-J. Ku, Y. Kim, *Thin Solid Films* **1997**, *304*, 222.

[8] G. A. Battiston, G. Carta, G. Cavinato, R. Gerbasi, M. Porchia, G. Rossetto, *Chem. Vap. Dep.* **2001**, *7*, 69.

[9] I. Bennett, R. Stevens, *British Ceramic Trans.* **1998**, *97*, 117; K. Wolf, DE-OS 2358663 **1975**; W. C. Ziegenhain, R. L. Poe, L. L. Bendig, J. F. Scamehorn, US Pat. 4133871 **1979**.

[10] G. W. Wagner, L. R. Procell, R. J. O'Connor, S. Munavalli, C. L. Carnes, P. N. Kapoor, K. J. Klabunde, *J. Am. Chem. Soc.* **2001**, *123*, 1636.

[11] C. L. Carnes, P. N. Kapoor, K. J. Klabunde, J. Bonevich, *Chem. Mater* **2002**, *14*, 2922.

[12] A. I. Kozlov, M. C. Kung, W. M. Xue, H. H. Kung, *Angew. Chem.* **2003**, *115*, 2517; *Angew. Chem. Int. Ed. Engl.* **2003**, *42*, 2415.

[13] G. H. Posner, D. Z. Rogers, *J. Am. Chem. Soc.* **1977**, *99*, 8208; G. H. Posner, D. Z. Rogers, *J. Am. Chem. Soc.* **1977**, *99*, 8214; Y. Harrak, M. D. Pujol, *Tetrahedron Lett.* **2002**, *43*, 819.

[14] M. Karpf, R. Trussardi, *J. Org. Chem.* **2001**, *66*, 2044.

[15] D. A. Atwood, J. A. Jegier, S. Liu, D. Rutherford, P. Wei, R. C. Tucker, *Organometallics.* **1999**, *18*, 976.

[16] M.-A. Munoz-Hernandez, P. Wei, S. Liu, D. A. Atwood, *Coord. Chem. Rev.* **2000**, *210*, 1.

[17] D. A. Atwood, Eur. Pat. 869103 **1998**.

[18] J. H. Wengrovius, M. F. Garbauskas, E. A. Williams, R. C. Goint, P. E. Donahue, J. F. Smith, *J. Am. Chem. Soc.* **1986**, *108*, 982.

[19] Measured in DMSO: R. Duchateau, U. Cremer, R. J. Harmsen, S. I. Mohamud, H. C. L. Abbenhuis, R. A. Van Santen, A. Meetsma, S. K.-H. Thiele, M. F. H. Van Tol, M. Kranenburg, *Organometallics.* **1999**, *18*, 5447.

[20] The Al–O–Al bond energy is typically in the range of 80–150 kJ mol^{-1}: J. P. Oliver, R. Kumar, *Polyhedron* **1990**, *9*, 409.

[21] D. A. Atwood, M. S. Hill, J. A. Jegier, D. Rutherford, *Organometallics.* **1997**, *16*, 2659; P. Wei, D. A. Atwood, *J. Organomet. Chem.* **1998**, *563*, 87.

[22] A. W. Apblett, A. C. Warren, A. R. Barron, *Can. J. Chem.* **1992**, *70*, 771.

[23] J. A. Wang, X. Bokhimi, A. Morales, O. Novaro, T. López, R. Gòmez, *J. Phys. Chem. B* **1999**, *103*, 299.

[24] C. Pecharromán, I. Sobrados, J. E. Iglesias, T. Gonzàlez-Carreño, J. Sanz, *J. Phys. Chem. B* **1999**, *103*, 6160.

[25] T. Tsuchida, N. Ichikawa, *Reactivity of Solids* **1989**, *7*, 207.

[26] C. H. Shek, J. K. L. Lai, T. S. Gu, G. M. Lin, *Nanostruct. Mater.* **1997**, *8*, 605.

[27] H.-M. Kao, R.-R. Wu, T.-Y. Chen, Y.-H. Chen, C.-S. Yeh, *J. Mater. Chem.* **2000**, *10*, 2802; G. Kunath-Fandrei, T. J. Bastow, J. S. Hall, C. Jaeger, M. E. Smith, *J. Phys. Chem.* **1995**, *99*, 15138.

[28] J. J. Fitzgerald, *ACS Symp. Ser.* **1999**, *717*.

[29] S. E. Ashbrook, K. J. D. MacKenzie, S. Wimperis, *Solid State Nucl. Magn. Reson.* **2001**, *20*, 87.

[30] R. C. T. Slade, J. C. Southern, I. M. Thompson, *J. Mater. Chem.* **1991**, *1*, 563.

[31] C. Morterra, C. Emanuel, G. Cerrato, G. Magnacca, *J. Chem. Soc., Faraday Trans.* **1992**, *88*, 339; K. A. Wickersheim, G. K. Korpi, *J. Chem. Phys.* **1965**, *42*, 579.

[32] L. D. Frederickson, Jr., *Anal. Chem.* **1954**, *26*, 1883.

[33] H. D. Ruan, R. L. Frost, J. T. Kloprogge, *J. Raman Spectros.* **2001**, *32*, 745.

[34] C. J. Harlan, M. R. Mason, A. R. Barron, *Organometallics.* **1994**, *13*, 2957.

